Simultaneous Measurement of Multiple Power Amplifiers for Phased Array Digital Predistortion Using a Shared Dual-Output Feedback

Bilal Khan, Nuutti Tervo, Rehman Akbar, Marko E. Leinonen, Olli Kursu, Aarno Pärssinen, and Markku Juntti
University of Oulu, Faculty of Information Technology and Electrical Engineering (ITEE)
{firstname.lastname}@oulu.fi

***Abstract*— Digital linearization of a phased array transmitters is usually based on feedback measurements. Various arrangements can be used to measure multiple transmit paths by using conducted or radiated methods. We propose a technique for measuring any pair of transmit paths simultaneously by using a common feedback connected to two receivers, and a cancellation method that can make the measurements independent. Together with the feedback cancellation, a single feedback line with two output ports can be used to measure different transmit chain pairs coherently under varying load conditions present in phased arrays. The cancellation filters are trained by using a fifth-generation (5G) new radio waveform and verified by over-the-air (OTA) measurements along with the predistortion performance evaluation of a 28 GHz 8-element phased array transmitter. The method achieved 30 dB cancellation between the paths and the DPD trained with the feedback cancellation achieved 4.2 % EVM and -40.8 dBc ACPR.**

***Keywords*— Antenna array, digital predistortion (DPD), power amplifier (PA) linearization, Feedback receiver.**

I. Introduction

Phased arrays are the dominant approach to enable millimeter-wave communications in fifth-generation (5G) [1] and sixth-generation (6G) [2] systems. For achieving good efficiency and transmit power, the power amplifiers (PAs) of the phased array transmitter (Tx) are operated in their nonlinear region. However, the nonlinear distortion of the PA reduce the signal quality and cause interference to the users in adjacent frequency bands.

The PA nonlinearity is often pre-corrected by a digital predistortion (DPD) that is based on feedback receiver (Rx) measurements. However, in phased arrays, multiple PAs have to be measured to produce coefficients for a shared DPD linearizer. The DPD object formulation relies on the measurements, which are performed either through conductive [3]–[7], or over-the-air (OTA) methods [8], [9]. The conductive measurements can use, for example, time-shared approach, where the Rx is switched to access individual PA output one-by-one. However, due to the time-sharing, the measurement time is proportional to the number of parallel PAs. On the other hand, using OTA measurements require external antenna or antennas to measure the array response in near-field or far-field. OTA measurements offer a simplified solution, but the measurements are direction-dependent [4].

An architecture where multiple PAs share the same meandering microstrip used as a feedback path was presented in [3], [4]. The architecture used time-division duplex (TDD) switches to enable PAs one-by-one and the outputs were measured from the feedback paths in different time instants. However, the method in [3], [4] was not able to measure multiple PAs simultaneously due to their uncontrollable summation in the feedback path. In this paper, we use the same feedback architecture but extend the concept to measure multiple PA paths simultaneously by using digital cancellation filters between the two output ports of the feedback path. A phased array transmitter using the shared feedback path and feedback cancellation is presented in Fig. 1. The feedback path consists of two output ports that are connected to two coherent feedback receivers. The cancellation filters are trained based on single PA measurements. After the filter training, this feedback architecture along with the cancellation filters can be used to measure any PA pair in the presence of mutual coupling and antenna mismatches. Compared to other time-shared strategies, this can reduce the PA measurement time by half.

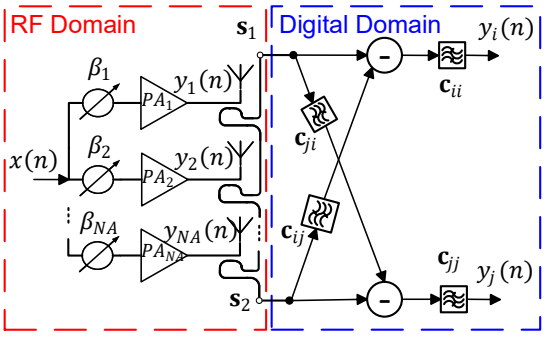

Fig. 1. Phased Array system diagram with feedback cancellation flow.

II. Shared Feedback and Cancellation Procedure for Measuring PA Pairs

When the PA output signals are coupled to the feedback path, they experience different attenuation and delay depending on the length of the path from the coupling point to the feedback output [4]. When two Tx paths are active simultaneously, their outputs combine in the feedback with different phases causing an arbitrary mixture of them in the feedback outputs. The feedback response from each coupled point to the output ports can be calibrated by using finite-impulse-response (FIR) filters as done in [4] for

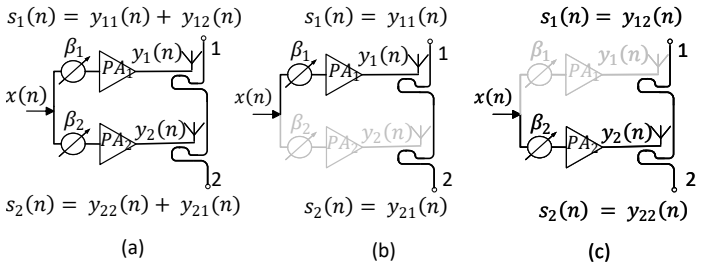

Fig. 2. Description of cancellation coefficient training. (a) PA-pair connected to the feedback line, (b) feedback outputs with PA1 active only, and (c) feedback outputs with PA2 active only.

individual PA measurements. Similarly, we can train the FIRs for multiple-PA measurements by using zero-forcing (ZF) over the feedback paths. The cancellation procedure over a PA-pair is explained in the following sections.

A. Feedback Cancellation Training

The flow chart of the proposed simultaneous PA-pair measurement approach is shown in Fig. 2. Fig. 2(a) shows two PAs sharing a feedback path with two output ports. $x(n)$ is a common input signal, $y_1(n)$ and $y_2(n)$ are the output of PA1 and PA2, respectively, and n is the sampling index. The aim is to extract $y_1(n)$ and $y_2(n)$ from the composite signals $s_1(n)$ and $s_2(n)$ simultaneously. The feedback path segments, that the PA output signals traverse, can be approximated by FIR filters trained by additional calibration measurements. The training mechanism is as follows: When PA1 is active only as shown in Fig. 2(b), the signals at the output ports are

$$s_1(n) = y_{11}(n), \tag{1}$$

$$s_2(n) = y_{21}(n) = \sum_{q=1}^{Q} c_{21}(q) y_{11}(n-q). \tag{2}$$

The FIR filter coefficients c_{21} can be estimated through Least-Square (LS) fitting as

$$\mathbf{c}_{21} = ({\mathbf{Y}_{11}}^H \mathbf{Y}_{11})^{-1} {\mathbf{Y}_{11}}^H \mathbf{Y}_{21} \tag{3}$$

where $\mathbf{Y}_{11} \in \mathbb{C}^{N \times Q}$ include all the basis functions of $\sum_{q=1}^{Q} y_{11}(n-q)$, $\mathbf{Y}_{21} \in \mathbb{C}^{N \times 1}$ is the signal measured at port 2 when only PA1 is active, N is the number of time domain samples, and $(.)^H$ denotes the Hermitian transpose. $\mathbf{c}_{21} = [c_{21,1}, c_{21,2}, ..., c_{21,Q}]$, $\mathbf{c}_{21} \in \mathbb{C}^Q$ denotes the FIR filter coefficient vector, and Q is the total number of coefficients. Similarly, when PA2 is active only as shown in Fig. 2(c), the signals at the output ports are

$$s_1(n) = y_{12}(n) = \sum_{q=1}^{Q} c_{12}(q) y_{22}(n-q), \tag{4}$$

$$s_2(n) = y_{22}(n), \tag{5}$$

where

$$\mathbf{c}_{12} = ({\mathbf{Y}_{22}}^H \mathbf{Y}_{22})^{-1} {\mathbf{Y}_{22}}^H \mathbf{Y}_{12}, \tag{6}$$

and $\mathbf{Y}_{22} \in \mathbb{C}^{N \times Q}$ include all the basis function of $\sum_{q=1}^{Q} y_{22}(n-q)$, $\mathbf{Y}_{12} \in \mathbb{C}^{N \times 1}$ is the signal measured at port 1 when only PA2 is active. $\mathbf{c}_{12} = [c_{12,1}, c_{12,2}, ..., c_{12,Q}]$, $\mathbf{c}_{12} \in \mathbb{C}^Q$ denotes the FIR filter coefficient vector. When both PAs are active at the same time, the signal at the output ports are

$$s_1(n) = y_{11}(n) + \sum_{q=1}^{Q} c_{12}(q) y_{22}(n-q), \tag{7}$$

$$s_2(n) = y_{22}(n) + \sum_{q=1}^{Q} c_{21}(q) y_{11}(n-q), \tag{8}$$

In (7), the additional signal component resulting from PA2 needs to be cancelled and same for (8). The cancellation flow is shown in Fig. 1. This cancellation is carried out in the digital domain. For cancellation we need to calculate the $\mathbf{c}_{11}$ and $\mathbf{c}_{22}$ coefficients. The output of the cancellation process of Fig. 1 is given by

$$\mathbf{y}_1 = (\mathbf{s}_1 - \mathbf{s}_2 \circledast \mathbf{c}_{12}) \circledast \mathbf{c}_{11}, \tag{9}$$

$$\mathbf{y}_2 = (\mathbf{s}_1 - \mathbf{s}_2 \circledast \mathbf{c}_{21}) \circledast \mathbf{c}_{22}, \tag{10}$$

where $\circledast$ denotes convolution. Putting (7) and (8) in (9) and solving for $\mathbf{c}_{11}$ results in

$$\mathbf{y}_1 = (\mathbf{y}_{11} - \mathbf{y}_{21} \circledast \mathbf{c}_{12}) \circledast \mathbf{c}_{11}, \tag{11}$$

Note that in the training stage, the output of PA1 i.e., $\mathbf{y}_1$ can be measured through an OTA RX antenna. Similarly, $\mathbf{y}_{11}$ and $\mathbf{y}_{21}$ are measured through feedback output ports, when only PA1 is active. The FIR filter coefficients $\mathbf{c}_{11}$ can be estimated through LS fitting as

$$\mathbf{c}_{11} = (\mathbf{A}^H \mathbf{A})^{-1} \mathbf{A}^H \mathbf{Y}_1 \tag{12}$$

Similarly, put (7) and (8) in (10) and solving for $\mathbf{c}_{22}$ results in

$$\mathbf{c}_{22} = (\mathbf{B}^H \mathbf{B})^{-1} \mathbf{B}^H \mathbf{Y}_2 \tag{13}$$

where $\mathbf{A}$ and $\mathbf{B} \in \mathbb{C}^{N \times Q}$ include all the basis functions of $(\mathbf{y}_{11} - \mathbf{y}_{21} \circledast \mathbf{c}_{12})$ and $(\mathbf{y}_{22} - \mathbf{y}_{12} \circledast \mathbf{c}_{21})$ respectively. $\mathbf{c}_{11}$ and $\mathbf{c}_{22} \in \mathbb{C}^Q$ denotes the FIR filter coefficient vectors.

After the feedback cancellation filters are trained, the PA responses can be measured simultaneously. The cancellation filters are applied in the digital domain to the composite signals $s_1(n)$ and $s_2(n)$ resulting from the active PA pair, and individual PA responses are extracted. It is worth noting that the composite signals include the impact of mutual coupling between the active PA branches and antenna mismatches. By using this approach, any i, j PA-pair can be measured simultaneously through the shared feedback path in one measurement round, and thus, potentially reducing the measurement time by half.

III. Experimental Verification with Array DPD

A. Measurement Setup

The demonstration platform used in our analysis is a 28 GHz transceiver module with Gallium Nitride (GaN) PAs [4], [10]. This platform is equipped with 16 parallel PA-branches, out of which only 8 branches are used in this paper. The PA-branches share an

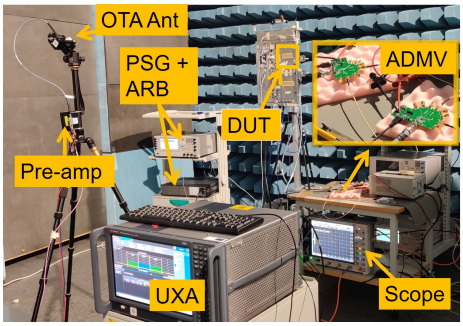

Fig. 3. OTA measurement setup in an anechoic chamber

integrated feedback path with two output ports as depicted in Fig. 1. The feedback output signals are received and down-converted to intermediate-frequency (IF) through ADMV1014 down-converters and are fed to Keysight DSOS104A oscilloscope. A photograph of the measurement setup in an anechoic chamber is shown in Fig. 3. A 100 MHz wide, 64 QAM cyclic-prefix (CP)-OFDM is fed to the IF input of the DUT by Keysight M8190A arbitrary-waveform-generator (ARB) and E8257B PSG. The received signals are acquired from oscilloscope in Matlab, and the feedback cancellation filters are applied to extract PA-branch responses. Furthermore, an additional OTA RX is used once in a training phase, and then the same OTA RX is used for DPD performance evaluation. In the OTA RX, we use a CA2630-141 pre-amplifier and A-info LB-28-15 standard gain horn antenna.

B. Measurement Results

1) Feedback Cancellation Performance for a PA-pair

Fig. 4 shows the feedback cancellation performance when the trained filter coefficients are applied to the composite signals at the feedback output ports. Figs. 4(a) and (b) shows PA1 and PA2 responses at both feedback outputs, respectively. For obtaining PA1 response, the aim is to extract it from feedback port 1 and suppress at feedback port 2. For PA2, the aim is opposite. Figs. 4(a) and (b) shows close to 30 dB cancellation between the individual PAs by using the proposed method. Fig. 4(c) shows the estimated array response of 2 elements from the composite signals at feedback ports in comparison to the array response measured OTA. The normalized-average-square-error (NASE) of the estimation of the array response of 2 elements is in the range of -26 to -30 dB for all PA-pairs of the array. The NASE is limited by the SNR of the signals at the feedback output ports.

2) DPD Performance of 8-element ULA

By using the feedback cancellation method, we trained a DPD for eight-element array in four groups of two PAs. The groups were chosen such that the adjacent PAs were active at a time. The obtained PA-branch responses from each PA-pair measurements are phase coherently combined to form an array response. The array response is used to calculate the DPD coefficients. The predistorter model used is a memory-polynomial (MP) model with the order of polynomial $K = 9$ and memory depth $M = 3$. The predistorter coefficients are calculated as

$$x(n) = \sum_{\substack{k=1 \\ k=\text{odd}}}^{K} \sum_{m=1}^{M} d_{k,m} y_{\text{array}}(n-m)|y_{\text{array}}(n-m)|^{(k-1)}, \quad (14)$$

where $y_{\text{array}}(n)$ is the array response obtained by combining the extracted PA-branch responses and $x(n)$ is the common input signal to the DPD. The problem can be written into matrix form and solved by least squares (LS) estimation as

$$\mathbf{d} = (\mathbf{Y}_{\text{array}}^H \mathbf{Y}_{\text{array}})^{-1} \mathbf{Y}_{\text{array}}^H \mathbf{x}, \quad (15)$$

where $\mathbf{d} = [d_{1,1}, d_{1,2}, ..., d_{1,M}, ..., d_{K,M}]$, $\mathbf{d} \in \mathbb{C}^{KM \times 1}$ denotes the DPD coefficient vector and $\mathbf{Y}_{\text{array}} \in \mathbb{C}^{N \times KM}$ include all the product terms of $\sum_{\substack{k=1 \\ k=\text{odd}}}^{K} \sum_{m=1}^{M} y_{\text{array}}(n-m)|y_{\text{array}}(n-m)|^{(k-1)}$ of (14).

For comparison against the proposed DPD method, we consider two other cases: i) OTA-DPD1, where the DPD is trained from array response measured with a reference antenna when all PA-branches are active simultaneously, and ii) OTA-DPD2, where the DPD is trained with reference antenna measurements but only single PA active at a time. Note that OTA-DPD2 does not take into account the impacts of mutual coupling. Fig. 5 shows the measured radiated signal spectrum in the main lobe for different DPD methods. The OTA-DPD1 is used as a reference scenario, against which the other two DPD methods are compared. From the figure, the OTA-DPD2 performance is worse because the DPD object was constructed based on individual PA-branch measurements in different time instants. Therefore, it does not take into account the impact of mutual coupling among the simultaneously active PAs, which potentially changes the nonlinear behavior of the PA-branches. Furthermore, the proposed DPD method provides comparable performance to that of the OTA-DPD1. The proposed method is based on PA pair measurements, and thus, taking into account the potential mutual coupling impacts of the adjacent PAs. In addition, the proposed DPD method also reduces the training time by half as two PA-branches are measured in one time instant.

The performance of the presented DPD methods in terms of adjacent-channel-power-ratio (ACPR), error-vector-magnitude (EVM), and effective-isotropic-radiated-power (EIRP) are combined in Table 1. The proposed DPD achieved -40.8 dBc ACPR and 4.2 % EVM measured in the main-lobe at 0° azimuth direction which is close to the performance of the DPD trained with a reference antenna in the main lobe. The 64-QAM signal constellation with and without the proposed DPD method is shown in Fig. 6.

Table 1. Main lobe ACPRs, EVM, and EIRP. Sub-indices L and H stands for lower and upper adjacent channels.

FOM	Without-DPD	OTA-DPD1	OTA-DPD2	Proposed
ACPR_L (dBc)	-29.73	-43.30	-36.06	-40.81
ACPR_H (dBc)	-32.70	-43.37	-42.11	-42.54
EVM (%)	9.7%	4.0%	4.8%	4.2%
EIRP (dBm)	42.5	42.4	42.3	42.4

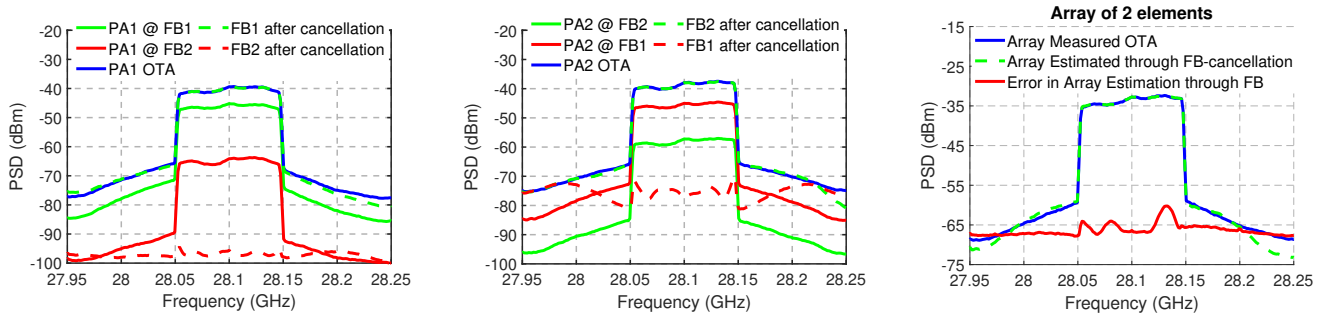

(a) (b) (c)

Fig. 4. Feedback (FB) cancellation performance. FB1 and FB2 stands for feedback ports. (a) PA1 response with and without feedback cancellation (b) PA2 response with and without feedback cancellation, and (c) Estimated response of 2 elements array through feedback path.

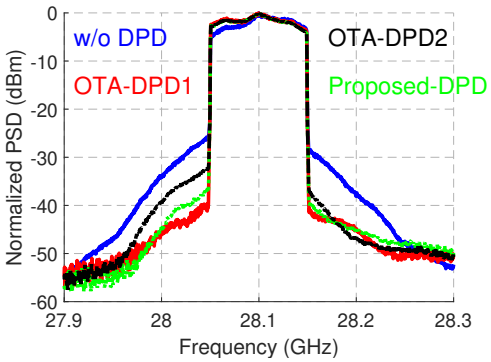

Fig. 5. Measured radiated signal spectrum in main lobe.

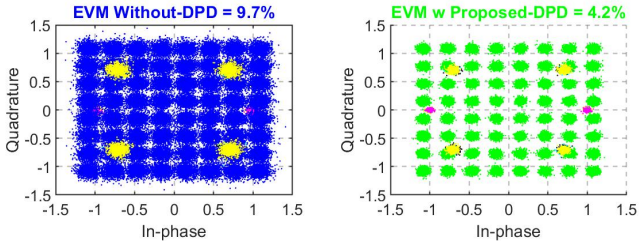

(a) (b)

Fig. 6. Main-lobe constellation of 64 QAM signal (a) Without-DPD and (b) With DPD using the proposed feedback cancellation.

IV. Conclusion

We proposed a feedback cancellation mechanism that allow simultaneous measurements of independent PA outputs using a single meandering feedback line with two output ports. The cancellation coefficients were trained by using additional calibration measurements where individual PAs were enabled one-by-one. After training the cancellation, the system was able to measure any pair of PAs simultaneously by a single dual-output feedback line. The cancellation performance was verified by using 5GNR signal. In the example case, the technique achieved 30 dB of cancellation between the paths. The cancellation was applied to an eight-element PA array in four groups of two PAs and a common DPD was trained. As a reference DPD method we used DPD trained with far-field reference antenna, and DPD trained from measurements with only a single PA active at a time. The proposed DPD achieved 4.2 %EVM and -40.8 dBc ACPR which was comparable to the DPD performance trained through a reference antenna and better than the DPD trained by individidual PA measurements in different time instants. The cancellation method can be applied in different conducted and OTA feedback architectures for training the calibration and digital predistortion of phased array transmitters.

Acknowledgment

This research work has been financially supported by Energy-Efficient Radio Access: Methods and Optimization (EERA) and Academy of Finland 6Genesis Flagship (grant no. 318927).

References

[1] T. S. Rappaport *et al.*, "Millimeter wave mobile communications for 5g cellular: It will work!" *IEEE Access*, vol. 1, pp. 335–349, 2013.

[2] M. Latva-aho and K. Leppänen, *Key drivers and research challenges for 6G ubiquitous wireless intelligence*. Oulu, Finland: University of Oulu, 2019.

[3] N. Tervo *et al.*, "Digital Predistortion of Millimeter-Wave Phased Array Transmitter With Over-the-air Calibrated Simplified Conductive Feedback Architecture," in *2020 IEEE MTT-S Int. Microw. Symp. (IMS)*, 2020, pp. 543–546.

[4] ——, "Digital Predistortion of Phased-Array Transmitter With Shared Feedback and Far-Field Calibration," *IEEE Trans. Microw. Theory Techn.*, vol. 69, no. 1, pp. 1000–1015, 2021.

[5] S. Lee *et al.*, "Digital Predistortion for Power Amplifiers in Hybrid MIMO Systems with Antenna Subarrays," in *2015 IEEE 81st Veh. Technol. Conf. (VTC Spring)*, 2015, pp. 1–5.

[6] X. Liu *et al.*, "Beam-Oriented Digital Predistortion for 5G Massive MIMO Hybrid Beamforming Transmitters," *IEEE Trans. Microw. Theory Techn.*, vol. 66, no. 7, pp. 3419–3432, 2018.

[7] S. Hesami *et al.*, "Single digital predistortion technique for phased array linearization," in *2019 IEEE International Symposium on Circuits and Systems (ISCAS)*, 2019, pp. 1–5.

[8] N. Tervo *et al.*, "Digital Predistortion Concepts for Linearization of mmW Phased Array Transmitters," in *2019 16th Int. Symp. Wireless Commun. Syst (ISWCS)*, 2019, pp. 325–329.

[9] E. Ng *et al.*, "Digital Predistortion of Millimeter-Wave RF Beamforming Arrays Using Low Number of Steering Angle-Dependent Coefficient Sets," *IEEE Trans. Microw. Theory Techn.*, vol. 67, no. 11, pp. 4479–4492, 2019.

[10] O. Kursu *et al.*, "Design and Measurement of a 5G mmW Mobile Backhaul Transceiver at 28 GHz," *EURASIP Journal on Wireless Communications and Networking*, vol. 2018, 12 2018.